Arrayed rGO_{SH}/PMA_{SH} Microcapsule Platform Integrating Surface Topography, Chemical Cues, and Electrical Stimulation for Three-Dimensional Neuron-Like Cell Growth and Neurite Sprouting

Heng-Wen Liu, Wei-Chen Huang, Chih-Sheng Chiang, Shang-Hsiu Hu, Chia-Hsin Liao, You-Yin Chen, and San-Yuan Chen**

The biocompatible thiol-functionalized rGO_{SH}/PMA_{SH} microcapsules encapsulating nerve growth factor (NGF) are arrayed onto a transparent and conductive substrate, i.e., indium tin oxide (ITO), to integrate electrically stimulated cellular differentiation, electrically controlled NGF release, and topographically rough nano-surfaces into a 3-D platform for nerve regeneration. The rGO_{SH}/PMA_{SH} microcapsules with microscale topography function not only as an adhesive coating to promote the adhesion of PC12 cells but also as electroactive NGF-releasing electrodes that stimulate NGF release and accelerate the differentiation of PC12 cells during electrical stimulation. Once electrical treatment is applied, NGF release and electrically enhanced cellular differentiation lead to an obvious increase both in the percentage of cells with neurites and in the neurite length. This length can reach nearly 90 μm within 2 days of cell culture. The average neurite length is significantly increased (four-fold) after culture on the rGO_{SH}/PMA_{SH} microcapsule substrate for 2 days compared with culture on a substrate without an rGO_{SH}/PMA_{SH} coating. These multifunctional rGO_{SH}/PMA_{SH} microcapsules may be used as potential 3-D patterned substrates for neural regeneration and neural prosthetics in tissue engineering applications.

1. Introduction

The interfaces between material surfaces and cells play important roles in cell functions, including adhesion, proliferation, and differentiation. Many studies have reported that topographical features can be used to stimulate cells to guide and enhance cell performance.[1] Topographical surfaces with microscale roughness were reported to have particular use in neural cell growth because entire neurites can be trapped within the microstructures, restricting the direction of neurite growth or generating tension at the cellular level.[2,3] This strategy has been employed by designing and coating novel materials[4] to increase surface roughness, immobilize cells, and enhance cell differentiation. Additionally, electrical stimulation is crucial for increasing the number of cells with neurites or shortening the differentiation time.[5] This stimulation can be achieved by coating with conducting materials, such as carbon nanotubes,[6] a conducting polymer,[7] or potentially previously unused materials. Moreover, the incorporation of neuronal guidance and drugs in materials can increase cell performance.[8] Certain studies grafted nerve growth factor (NGF) onto the nerve guide structure or encapsulated NGF in polymeric microspheres[9] for delivery.[2,10] However, to the best of our knowledge, most platforms cannot seal great amounts of growth factor into spheres and control its release precisely in real time, which may lead to undesirable release, causing a low efficiency of cellular growth and differentiation. The integration of precisely controlled neuron/material interfaces with multifunctionality and guidance modalities (physical cues, chemical cues, and electrical stimulation) into a single platform to enhance cell growth and differentiation is one possible approach to rapidly reconnecting severed nerve ends.

The need to address this challenge stimulated us to design optimal scaffold architecture, including the use of new materials to design specialized and effective neural interfaces that

H.-W. Liu, W.-C. Huang, C.-S. Chiang, Prof. S.-Y. Chen
Department of Materials Science and Engineering
National Chiao Tung University, No. 1001
Ta-Hsueh Rd., Hsinchu, Taiwan 300, R.O.C
E-mail: sanyuanchen@mail.nctu.edu.tw
Prof. S.-H. Hu
Department of Biomedical Engineering
and Environmental Sciences
National Tsing Hua University
Hsinchu, Taiwan
Prof. C.-H. Liao
Department of Medical Research
Buddhist Tzu Chi General Hospital
No. 707, Sec. 3, Chung-Yang Rd., Hualien, Taiwan 970, R.O.C.
Prof. Y.-Y. Chen
Department of Biomedical Engineering
National Yang Ming University
No. 155, Sec. 2, Linong St., Taipei, Taiwan 112, R.O.C.
E-mail: irradiance@so-net.net.tw

DOI: 10.1002/adfm.201303853

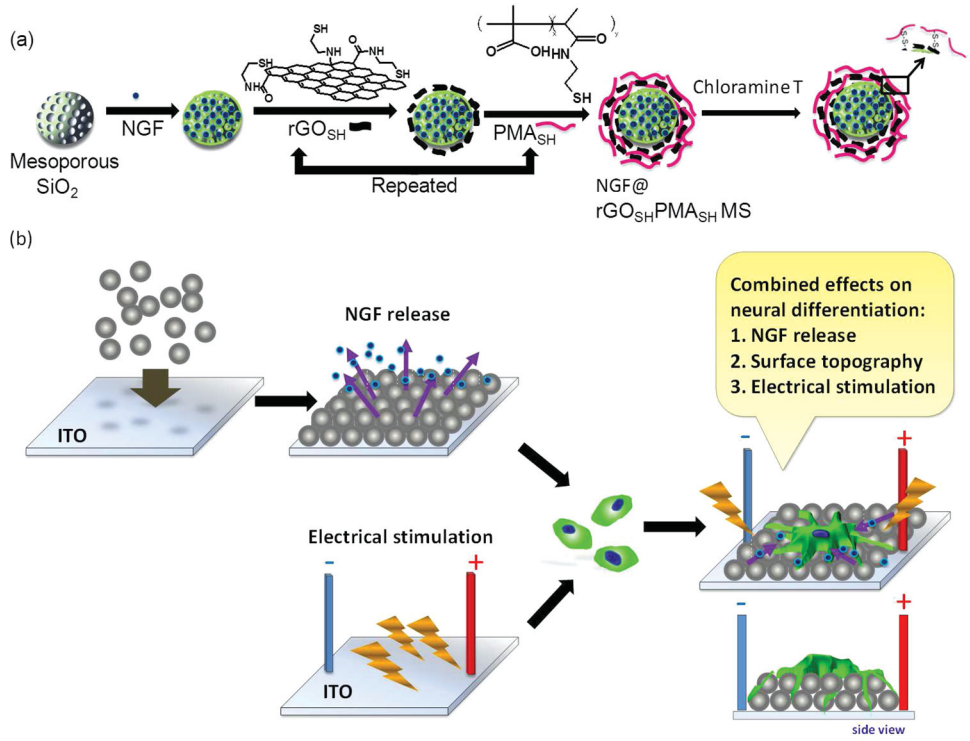

Figure 1. a) Preparation of rGO_{SH}/PMA_{SH} multilayers on the surface of MS particles by hydrogen bonding and formation of the disulfide linkages. b) Schematic diagram of rGO_{SH}/PMA_{SH} MS arrayed onto an ITO surface for nerve regeneration by electrical stimulation.

control neuronal development and neurite outgrowth. Recently, graphene and its derivatives, such as graphene oxide (GO) and reduced graphene oxide (rGO) sheets, have received great attention in biomaterial applications because of their outstanding electrical, mechanical, thermal, and biocompatible properties.[11] Using a simple layer-by-layer (LbL) assembly method, a two-dimensional graphene nanosheet can be developed into three-dimensional (3-D) functional materials. For example, Hong et al.[12] formed multilayer hollow graphene capsules using electrostatic interactions to produce $(rGO\text{-}NH_3^+/rGO\text{-}COO^-)_n$. Ju et al.[13] proposed a novel approach for the fabrication of positively charged polystyrene beads, or polymer nanospheres, coated with negatively charged graphene with electrical conductivity. The use of the LbL approach and graphene material to form hollow spheres has shown advantages over traditional capsule formulations. To address the present limitations in neuronal cell culture, our group combined a thiol polymer with rGO to provide a unique and suitable platform for neuron-like cells. A mesoporous microcapsule core with an rGO and polymer shell was designed and developed in this study to increase NGF encapsulation in the core, without decreasing electrical stimulation of the cells, and to enhance the surface roughness of the shell and its surface's affinity for cells. Furthermore, the substrate containing rGO-coated microcapsules has several advantages, particularly with regard to its flexibility in pattern coating, electrical characteristics, surface roughness, and cell activity.

Herein, we describe a graphene/polymer LbL microcapsule substrate for the integration of multiple cues into one structure that enhanced the differentiation of rat pheochromocytoma (PC12) cells. We first functionalized the thiol groups on poly(methacrylic acid) (PMA) as well as rGO; we then oxidized the thiol groups into disulfide linkages between the rGO_{SH} and PMA_{SH} chains within the multilayer to provide structural stability. These microcapsules made from the two-dimensional rGO nanosheet can promote NGF release under electrical stimulation due to electroosmosis coupled with electrophoresis.[14] Moreover, due to the deposition of rGO on the shell surface of the microcapsule to retain its intrinsic conductive nature, we can manipulate the proliferation and differentiation of PC12 cells by integrating electrical stimulation, surface roughness, and the NGF cue into one responsive, multifunctional rGO_{SH}/PMA_{SH} LbL microcapsule substrate. Based on our understanding of the interaction between PC12 cells and the rGO_{SH}/PMA_{SH} microcapsule substrate, we will apply this responsive substrate to neural regeneration and neural prosthetics through neural tissue engineering.

2. Results and Discussion

2.1. Synthesis of rGO_{SH}/PMA_{SH} Mesoporous Silica

Figure 1a schematically illustrates the preparation of rGO_{SH}/PMA_{SH} LbL microcapsules in which the preloading technique was conducted to encapsulate 90% of NGF (135 ng) in rGO_{SH}/PMA_{SH} microcapsules. The LbL shell acquired versatile functions by integrating inorganic and organic molecules. We used the small size of the rGO sheet to modify the thiol groups on its surface. The size of the rGO sheet was measured by DLS,

as shown in Figure S1 (see Supporting Information). Inorganic rGO_{SH} was used in this study based on its electrical properties, biocompatibility, and functionalized thiol groups, whereas organic PMA_{SH}, which has been widely used in LbL capsules in recent years,[15] was used due to its biocompatibility, hydrogen bond donors, and stability via disulfide linkages. The thiol-functionalized PMA (PMA_{SH}) is deposited alternately with rGO_{SH} on the the surface of amine-functionalized, positively charged mesoporous silica (MS) particles through the hydrogen bonding between PMA_{SH} and rGO_{SH}. The coating step was repeated to control the shell thickness and 6 bilayers of PMA_{SH}/rGO_{SH} were used in this study. After the conversion of the thiol groups into disulfide cross-links by chloramine T, an oxidative reagent, the LbL microcapsules became stable in the extracellular environment due to the disulfide bonds.

Figure 1b schematically shows the arrayed rGO_{SH}/PMA_{SH} MS as a growth factor reservoir that can be used to study release behavior from extracellular matrices and as a template that can be applied to improve PC12 cell proliferation and differentiation in response to an electrical stimulus. The microcapsule template combines the effects of surface topography, the NGF chemical cue, and electrical stimulation to enhance PC12 cell performance on this substrate.

2.2. Structural Morphology of rGO_{SH}/PMA_{SH} MS

The MS core particles displayed a structurally uniform morphology and had a mean particle size of 3 μm. **Figure 2**a displays an optical micrograph of the orderly configuration of the NGF-loaded rGO_{SH}/PMA_{SH} microcapsules on a transparent ITO substrate. In Figure 2b, SEM imaging of the rGO_{SH}/PMA_{SH} microcapsules further demonstrates that the dried particles were uniformly and compactly arranged on the ITO substrate. The self-assembly of these microcapsules on the ITO susbtrate was regulated and fixed by particle interactions through the solvent evaporation and 2-hydroxyethyl methacrylate (HEMA) polymerization processes. As the solvent evaporated slowly, the microcapsules were gathered together and arranged on the substrates to form 3-D structure as illustrated in Figure S2, Supporting Information. The enlarged SEM image in Figure 2c shows that the surface of the MS after assembly with rGO_{SH}/PMA_{SH} molecules displayed a rough texture, implying that the rGO_{SH} layer was adsorbed on polymer spheres. The coating quality was directly dependent on the concentration of PMA_{SH} and rGO_{SH}, the lateral length of the rGO_{SH} sheet, and the coating time. We repeatedly used ultracentrifugation with high-power ultrasonication to obtain a narrow size distribution of rGO_{SH} sheets, which were generally smaller than the diameter of the MS core. Although we precisely controlled the concentration and size to obtain individual particles that were homogeneously coated with PMA_{SH} and rGO_{SH}, a few rGO_{SH} sheets adhered to more than one sphere and formed a bridge linking nearby particles simultaneously, as shown in Figure 2c. The SEM image in Figure 2d shows the collapsed morphology of a sample after removing the MS core using HF/NH_4F, indicating that the LbL microcapsules exist in a hollow state. The rGO_{SH}/PMA_{SH} microcapsules' core shell structure is clearly

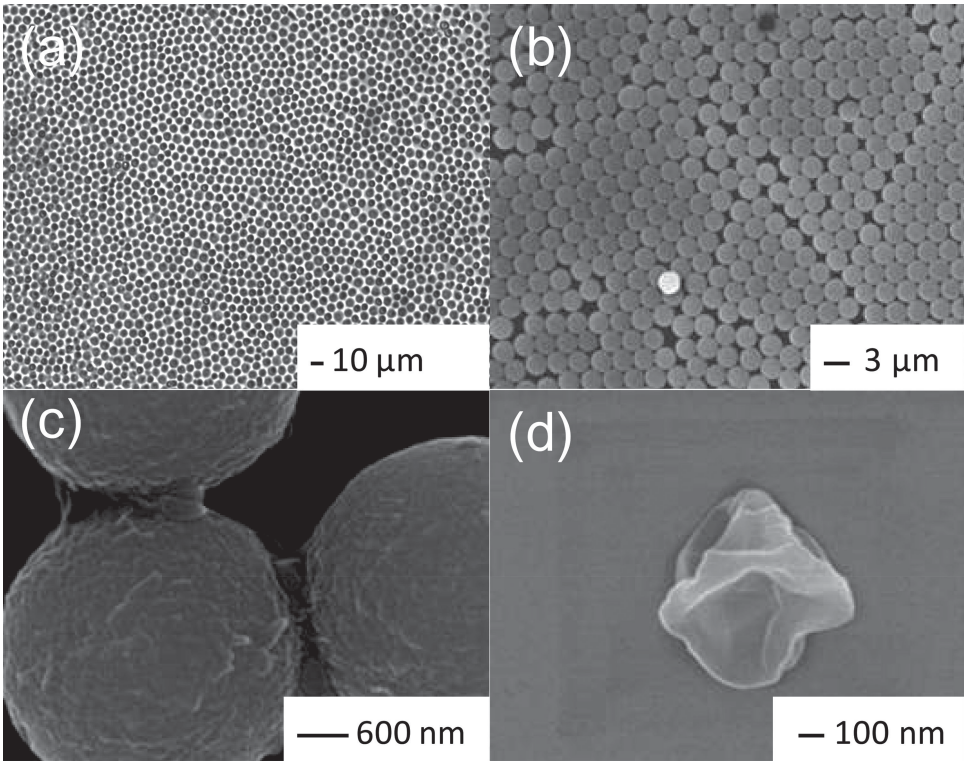

Figure 2. a) Optical micrograph of the arrayed microcapsules. b) SEM image of the rGO_{SH}/PMA_{SH} microcapsules. c) High-magnification SEM image of rGO_{SH}/PMA_{SH} microcapsules obtained from (b). d) A hollow rGO_{SH}/PMA_{SH} microcapsule.

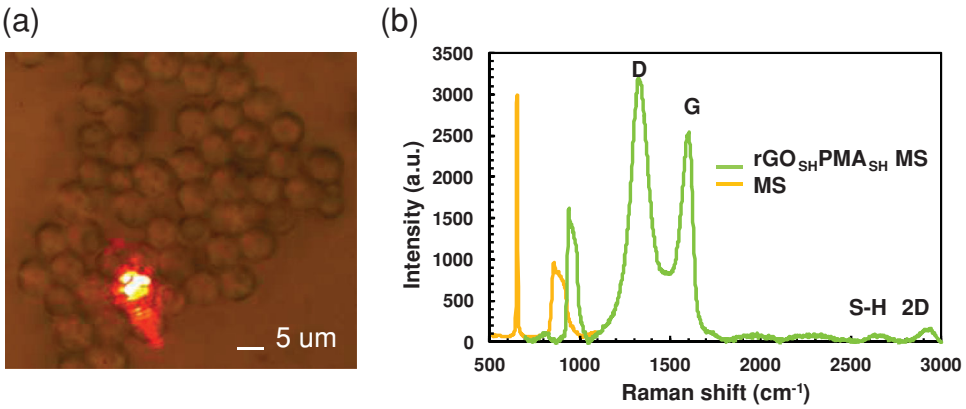

Figure 3. a) Optical microscopy images of laser-irradiated rGO_{SH}/PMA_{SH} microcapsules. The red spot in this figure indicates that the laser beam was focused on the rGO_{SH}/PMA_{SH} microcapsules. b) Raman spectrum of the MS and rGO_{SH}/PMA_{SH} microcapsules. The G-band and the D-band were attributed to the first-order scattering of the E_{2g} vibration mode in the graphite sheets and structural defects (disorder-induced modes), respectively. For the rGO_{SH}/PMA_{SH} microcapsules, the D-band was at 1322 cm^{-1}, the G-band was at 1602 cm^{-1}, the 2D-band was at 2918 cm^{-1}, and thiol (S-H) was at 2605 cm^{-1}.

shown in the PL microscopy images in Figure S3, Supporting Information.

2.3. Characterization of rGO_{SH}/PMA_{SH} Microcapsules

The size of the rGO sheet used for coating was measured by DLS, as shown in Figure S1, Supporting Information. To verify the coating of rGO onto the microcapsules, we used a Raman spectrometer coupled with an OM to evaluate the microcapsules before and after coating with rGO. As shown in **Figure 3**a, a laser beam was directly focused on the microcapsules. In Figure 3b, the Raman spectrum of the MS microcapsules displays only two peaks, one at 520 cm^{-1} and the other at 943 cm^{-1}, which are the first-order and the second-order phonon scattering of silica, respectively. The G-band and the D-band were attributed to the first-order scattering of the E_{2g} vibration mode in the graphite sheets and structural defects (disorder-induced modes), respectively. For the rGO_{SH}/PMA_{SH} microcapsules, the following were clearly observed: a D-band at 1322 cm^{-1}; a G-band, which had sp^2-hybridized carbon-carbon bonds,[16] at 1602 cm^{-1}; and a 2D-band, the overtone (second harmonic) of the D-band, at 2918 cm^{-1}. The relative ratio of D- to G-band intensity (I_D/I_G) was 1.24, which corresponds to the Raman spectrum of rGO. Moreover, the thiol groups on the rGO and PMA appeared at 2605 cm^{-1}. The results demonstrated that rGO and thiol molecules were successfully deposited and adsorbed on MS.

To assess whether the rGO_{SH}/PMA_{SH} MS substrate can retain the intrinsic electrical conductivity of rGO, we assessed the electrical conductivity of the rGO, rGO_{SH} and rGO_{SH}/PMA_{SH} MS substrates using the four-probe method. The rGO sheets, rGO_{SH} sheet and rGO_{SH}/PMA_{SH} MS showed electrical conductivities of 1.74, 1.62, and 1.01 S m^{-1}, respectively. Although a lower electrical conductivity was obtained with rGO_{SH}/PMA_{SH} MS, our study revealed that the electron transfer behavior still can occur in the substrate, even after the microcapsules are covered with PMA. After the rGO_{SH}/PMA_{SH} MS was subjected to cell culture and electrical stimulation for 1 h at 1 V at 2 days, the rGO_{SH} sheets became somewhat exposed in some places which were demonstrated on the SEM images in Figure S4, Supporting Information. The morphology indicated that the electrical stimulation still can be applied on the cells adhered on rGO_{SH}/PMA_{SH} due to the exposure of the rGO_{SH} sheet and bridge linking neighboring microcapsules. The possible mechanism can be illustrated in Figure S5, Supporting Information. When the $NGF@rGO_{SH}/PMA_{SH}$ MS substrate was exposed to the electric field, the mobile counter ions tended to migrate toward the cathode and drag water and NGF molecules with them. At the same time, the negatively charged rGO_{SH} sheets in the PMA_{SH} matrix may be subjected to an action toward the anode and exposed on the surface. The NGF release from the rGO_{SH}/PMA_{SH} MS substrate without and with electrical stimulation was further studied and is shown in Figure S6, Supporting Information. A greater NGF release was observed in the presence of electrical stimulation than with no electrical stimulation.

2.4. Evaluation of Cell Viability, Proliferation, and Differentiation in the Absence and Presence of Electrical Stimulation

To determine whether the microcapsule materials could act as suitable substrates, PC12 cells were grown for 1 or 4 days on the ITO, MS, and rGO_{SH}/PMA_{SH} MS substrates, after which the cells were fixed. The cell viability was measured using a live/dead viability/cytotoxicity kit (Molecular Probes, Eugene, OR). **Figure 4**a shows that the cell viability on the MS and rGO_{SH}/PMA_{SH} MS substrates after 1 day was 47 ± 8% and 53 ± 9%, respectively, which was slightly higher than the viability on the ITO substrate (43 ± 5%) at 1 day. There was no significant difference between the ITO and rGO_{SH}/PMA_{SH} MS substrates at 1 day. Moreover, an increased rate of effective cell viability was observed after 4 days when PC12 cells were cultured on the rGO_{SH}/PMA_{SH} MS substrate. We observed a significant difference ($^{**}P < 0.01$) in the cell viability between the ITO (66 ± 7%) and the rGO_{SH}/PMA_{SH} MS (99 ± 10%) substrates at 4 days. The rGO_{SH}/PMA_{SH} MS substrate greatly enhanced cell viability compared with the ITO and MS substrates. Representative

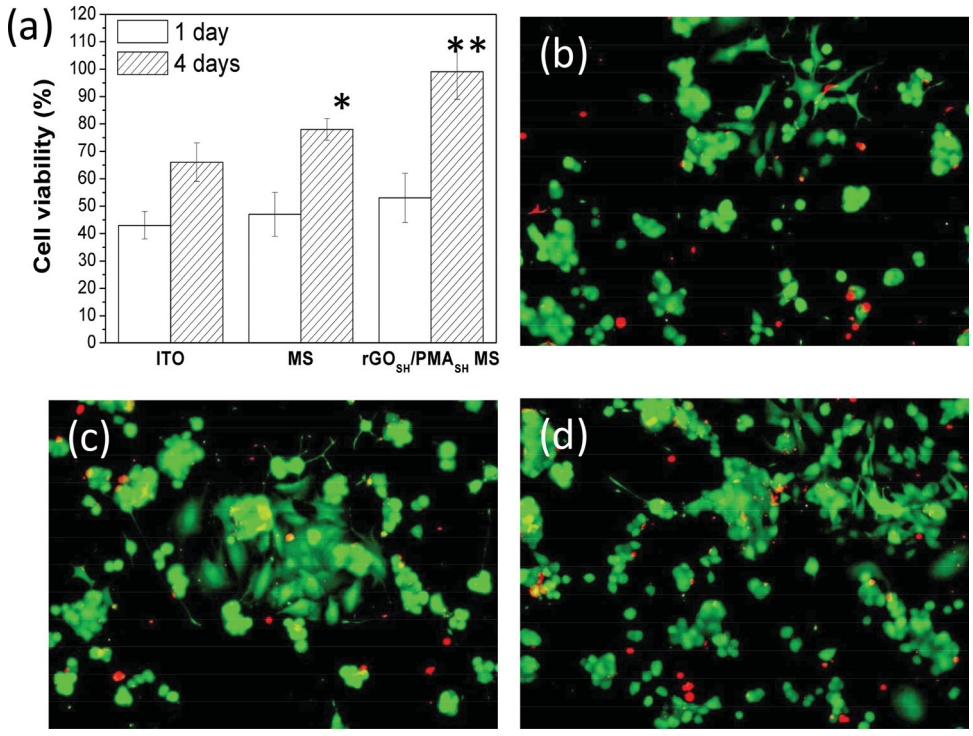

Figure 4. a) PC12 cell viability (%) using a live/dead assay at one day and four days. ($N = 5$) Data are presented as the mean ± SEM.$^{*}P < 0.05$ was considered statistically significant with respect to the MS substrate and ITO substrate after 4 days. $^{**}P < 0.01$ compared with the rGO$_{SH}$/PMA$_{SH}$ MS substrate and the ITO substrate after 4 days. b–d) Fluorescent (100×) images of live (calcein AM, green) and dead (ethidium homodimer-1, red) cells cultured for 4 days on b) ITO, c) MS, and d) rGO$_{SH}$/PMA$_{SH}$ MS substrates.

live/dead images of cells cultured on the ITO, MS, and rGO$_{SH}$/PMA$_{SH}$ MS substrate for 4 days are shown in Figure 4b–d. These observations provided evidence for the importance of using the rGO$_{SH}$/PMA$_{SH}$ MS substrate for the PC12 cell culture. An MTT assay[17,18] was also used to evaluate the cell viability in this study, as shown in Figure S7 (Supporting Information), which presents the consistent change of PC12 cell viability on the ITO, MS, and rGO$_{SH}$/PMA$_{SH}$ MS substrates compared with those measured by a fluorescent live/dead cell assay.

This trend is also apparent in Figure S8 (Supporting Information), which shows PC12 cell adhesion to and proliferation on the ITO and rGO$_{SH}$/PMA$_{SH}$ microcapsule substrates without electrical stimulation in the culture medium. These results imply that this rGO$_{SH}$/PMA$_{SH}$ MS substrate possesses high biocompatibility. The results can be attributed to the surface nanoroughness and the biocompatibility of rGO$_{SH}$/PMA$_{SH}$, which has been reported to enhance cellular adhesion and activity,[19] thereby leading to cell proliferation.[7,8] Furthermore, compared with other substrates, rGO nanosheets have an intrinsic advantage in building interfaces with cells and tissue and are thus a good raw material to support neuronal cell proliferation.[20] For example, Park et al.[21] suggested that graphene can be used as an excellent nanostructured scaffold for enhancing human neural stem cell adhesion and differentiation in the long term. Therefore, as expected, PC12 cells grew very well on these regions, indicating that rGO$_{SH}$/PMA$_{SH}$ MS does not have a harmful effect on PC12 cells compared with other cell-growth substrates, such as ITO and MS. Furthermore, the rGO$_{SH}$/PMA$_{SH}$ MS substrate provided an optimal rough surface structure for the enhancement of PC12 cell adhesion as well as proliferation.

We expanded this study to observe the effects of electrical stimulation on cell behavior on the ITO, MS, and rGO$_{SH}$/PMA$_{SH}$ MS substrates (22 mm × 22 mm) by applying a constant voltage of 1 V for 1 h. In this experiment, no NGF was added to the system; rather, only electrical stimulation was applied to each substrate. **Figure 5** quantifies the cell viability, the average neurite length and the number of cells with neurites after 2 days of electrical stimulation in Figure 5a–c, respectively. A P-value < 0.05 was considered to be statistically significant. Clearly, a substrate with electrical stimulation exhibited a statistically significant improvement in cell performance over the substrate without electrical stimulation.

Although the electrical effect on the cell viability was not significant, as shown in Figure 5a, PC12 cells showed slightly enhanced viability on the rGO$_{SH}$/PMA$_{SH}$ MS substrates. However, the enhancing effect of an electric field on differentiation has been reported by several publications.[22] The proportion of the neurite length and cells with neuriteswere greatly increased under an electric field, as shown in Figures 5b,c, compared with those on ITO because of the dominant surface topography. Moreover, the rGO$_{SH}$/PMA$_{SH}$ MS substrate still induced statistically significantly greater PC12 cell differentiation than did the MS substrate. This result indicates that PC12 cell activity can be largely enhanced on the rGO$_{SH}$/PMA$_{SH}$ MS substrate because the coating of rGO$_{SH}$ and PMA$_{SH}$ onto MS particles can increase surface roughness, conductivity, and biocompatibility. Consequently, MS with an rGO$_{SH}$/PMA$_{SH}$ coating offers major

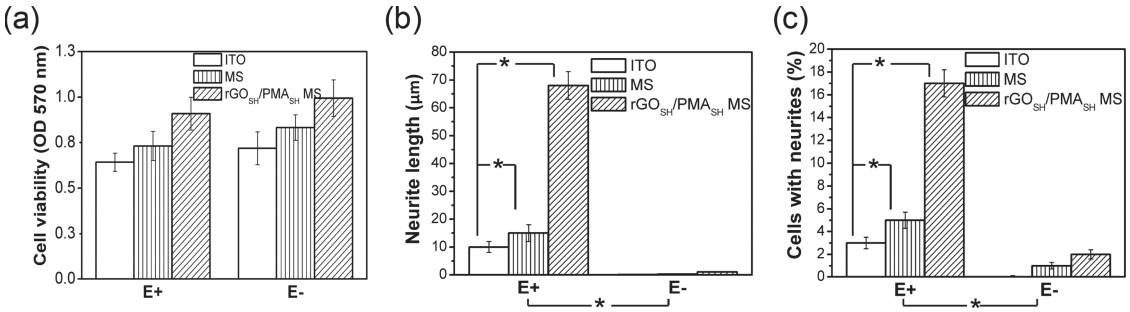

Figure 5. Cell behavior of PC12 cells attached on ITO, MS, and rGO_{SH}/PMA_{SH} MS substrates by electrical stimulation or not. a) Cell viability, b) the neurite length, and c) percentage of cells with neurites with and without electrical stimulation. PC12 cells were exposed to a constant voltage of 1 V for 1 h. For the rGO_{SH}/PMA_{SH} MS substrate under different conditions (NGF +: with NGF; NGF -: without NGF; E +: with electrical stimulation; E –: without electrical stimulation) ($N = 5$), $^{*}P < 0.05$ was considered statistically significant.

advantages over conventional flat ITO and non-coated MS as a neural interface.

2.5. Neuronal Changes of PC12 Cells Cultured on NGF-Loaded rGO_{SH}/PMA_{SH} Microcapsules Following Electrical Stimulation

The effects of the combined NGF cue and electrical stimulation on neuron markers of β-III-tubulin and neuron-specific cytoskeletal protein in PC12 cells cultured on the rGO_{SH}/PMA_{SH} microcapsules were observed by fluorescence and confocal imaging. **Figure 6**a shows representative fluorescence images of PC12 cells cultured on rGO_{SH}/PMA_{SH} microcapsules for 2 days in the presence of electrical stimulation. The cell nucleus was stained in blue, the actin cytoskeleton was stained in green, and the rGO_{SH}/PMA_{SH} microcapsules were stained in red to observe the neurite outgrowth and cell-matrix interaction. Based on the overlaid fluorescence images, we found much longer neurite extensions among PC12 cells cultured on rGO_{SH}/PMA_{SH} microcapsules. To further study the PC12 cell interaction with the arrayed microcapsules during electrical stimulation, cross-sectional confocal images were collected to understand the neurite outgrowth behavior. As shown in Figure 6(b), the neurite did not grow straight and seemed to interact with surface structures, such as trenches, microcapsule surfaces, and gaps between the microcapsules. PC12 cells were found to be well interconnected with the rGO_{SH}/PMA_{SH} microcapsules via the neurites of the cells. The longitudinal section also indicates that the neurites grew deep into the rGO_{SH}/PMA_{SH} microcapsules, whereas the nuclei remained above the microcapsules. The cross-sectional image shows that the neurites were widely splayed above the rGO_{SH}/PMA_{SH} microcapsules, directly indicating the high differentiation of the PC12 cells. The longest neurites achieved nearly 90 μm in length within 2 days of cell culture, which is much longer than the length reported by Cho et al. illustrating that PC12 cells grown on a Ppy/MSN-NGF composite substrate can possess neurites of approximately 20 μm in length after 2 days in culture.[23] In addition, Kang et al.[24] reported that NGF-loaded, 200-nm porous polypyrrole conducting polymers used as a substrate for PC12 cells can enhance neurite outgrowth to approximately 23 μm, which was much shorter than the neurites of PC12 cells cultured on our microcapsule substrate.

Figure 7 shows fluorescence images of PC12 cells cultured on rGO_{SH}/PMA_{SH} microcapsules imaged in a *z*-stack at depth intervals of 10 μm along the cross-section at each depth. In the first and second cross-sectional images, we observed that the

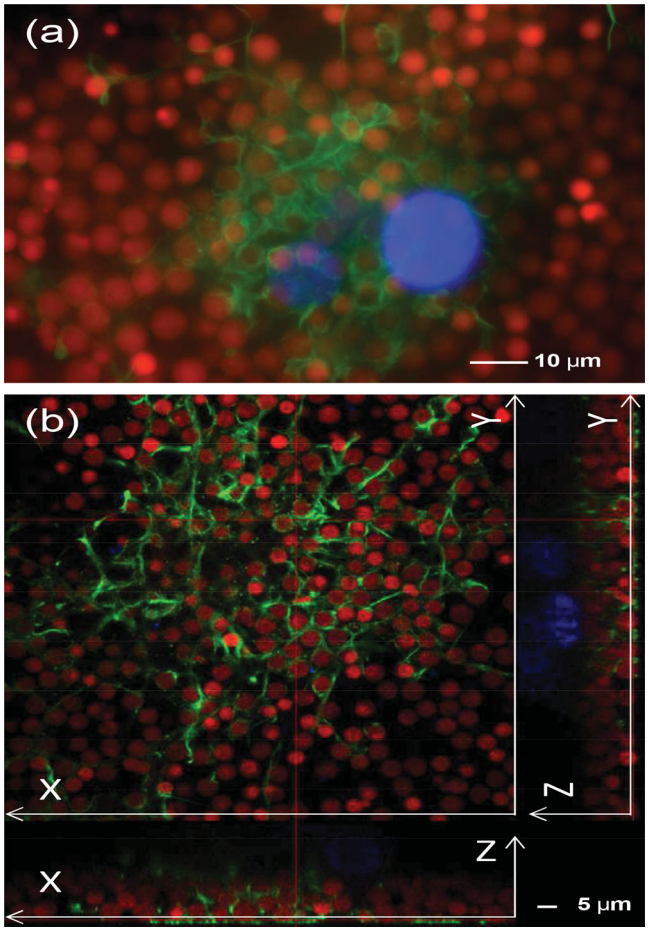

Figure 6. a) Low-magnification fluorescence images of PC12 cells adhered on rGO_{SH}/PMA_{SH} microcapsules after electrical stimulation for 2 days. b) Confocal microscopy images demonstrating that the electrical stimulation passed through the rGO_{SH}/PMA_{SH} microcapsules and then stimulated the PC12 cells to extend the neurite outgrowth into the rGO_{SH}/PMA_{SH} microcapsules. (red = microcapsules; green = β-III-tubulin/Alexa Fluor 488, cytoskeleton; blue = DAPI, nuclei).

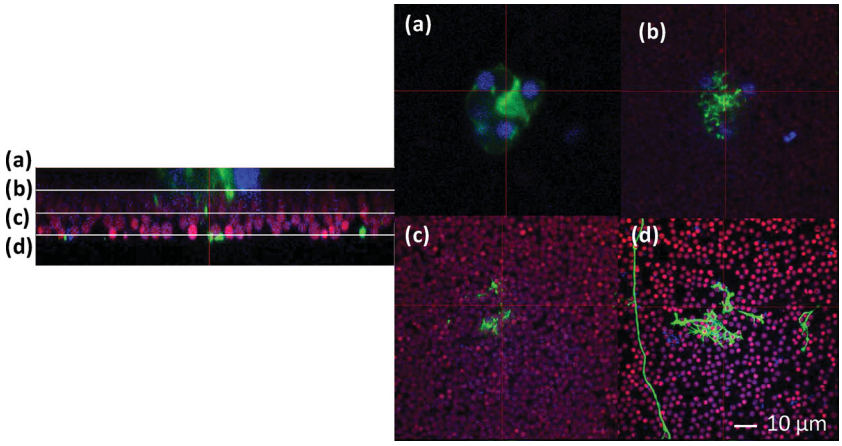

Figure 7. Confocal microscopy images of the neurite outgrowth of the PC12 cells that adhered onto surfaces of rGO_{SH}/PMA_{SH} microcapsules by electrical stimulation for 2 days. Positively expressed β-III-tubulin was observed in PC12 cells in the areas of the neurite that were extended in response to the combined NGF cue and electrical stimulation. The entire culture system was imaged in a *z*-stack at depth intervals of 10 μm along the cross-section at each depth (red = microcapsules; green = β-III-tubulin/Alexa Fluor 488, cytoskeleton; blue = DAPI, nuclei).

cell nuclei were above the arrayed rGO_{SH}/PMA_{SH} microcapsules. Neurites adhered to and extended into the microcapsules in the following intervals (the third and fourth cross-sectional images). Certain healthy neurites even extended into the deeper part and sprouted filopodial (microspikes) extensions toward the arrayed rGO_{SH}/PMA_{SH} microcapsules. It was noted that the neurites could grow in a particular downward direction when cultured on the arrayed rGO_{SH}/PMA_{SH} microcapsules, which served as a 3-D platform for the PC12 cells and guided the subsequent directional neurite growth of PC12 cells. Such surface guidance of cells can be employed toward the repair and regeneration of the nervous system. This result also suggested that a combined effect of surface topography, a chemical cue, and electrical stimulation can enhance neurite extension. Therefore, the NGF-loaded rGO_{SH}/PMA_{SH} microcapsules showed a positive effect on cell viability, proliferation, and differentiation because of the combined effects of the surface topography of the arrayed microcapsules, NGF release, and electrical stimulation. More importantly, when electrical stimuli were applied, greatly enhanced neurite outgrowths were detected in response to the increased differentiation. The success in inducing neurite growth with a longer length in the NGF-loaded rGO_{SH}/PMA_{SH} microcapsule system is promising for the further investigation of neural regenerative medicine for long axonal connections.

2.6. Effect of NGF Release on Cell Viability, Proliferation, and Differentiation in the Absence and Presence of Electrical Stimulation

We continued to evaluate neuron differentiation and neurite outgrowth by combining electrical, chemical, and surface topographical cues. Thus, we used the rGO_{SH}/PMA_{SH} MS substrate to study the effects of NGF encapsulation and electrical stimulation on cell behavior by co-culture with PC12 cells under different stimulated conditions, including with/without electrical stimulation and with/without NGF encapsulation in rGO_{SH}/PMA_{SH} MS. The cell viability, the neurite length, and the percentage of cells with neurites at 2, 4, and 7 days are shown in **Figures 8**a–c, respectively. There was no significant difference ($P > 0.05$) in cell viability between NGF-encapsulating and non-NGF-encapsulating rGO_{SH}/PMA_{SH} MS substrates by electrical stimulation or not after 2 days as shown in Figure 8a. At 4 days, the cell viability on the NGF@rGO_{SH}/PMA_{SH} MS substrate without/with electrical stimulation showed no significant difference, as shown in Figure 8(a), even though NGF was released at 25 ng and 111 ng, respectively, as shown in Figure S6. In addition, during 7 days of cell culturing, the cell viability

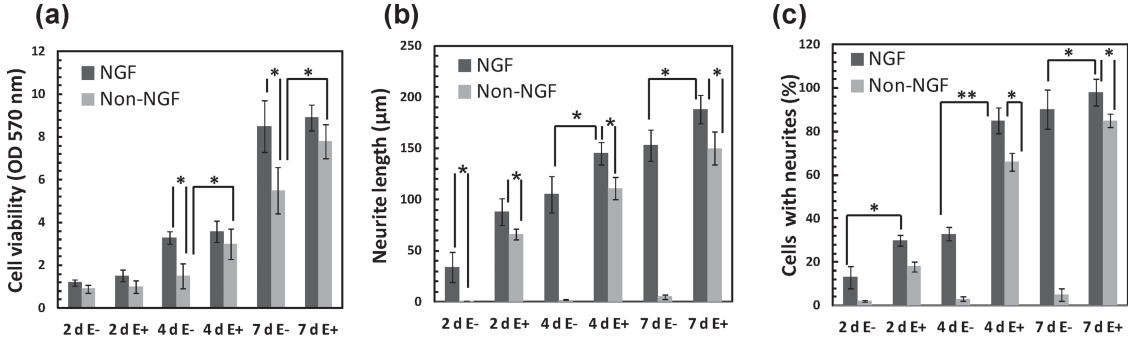

Figure 8. Comparison of PC12 cell behavior on NGF-encapsulating and non-encapsulating rGO_{SH}/PMA_{SH} MS substrates with and without electrical stimulation at 2, 4, and 7 days. a) Cell viability, b) the neurite length, and c) the percentage of cells with neurites of PC12 cells There was no significant difference ($P > 0.05$) in cell viability for NGF-encapsulating rGO_{SH}/PMA_{SH} MS substrates by electrical stimulation or not after 2, 4, and 7 days. There were apparent differences ($P > 0.05$) in cell viabilities for non-NGF-encapsulating rGO_{SH}/PMA_{SH} MS substrates when submitted to electrical stimulation after 4 and 7 days, respectively. Importantly, a significant enhancement of cell viabilities ($P < 0.05$) was found for the respective time points when PC12 cells received the simultaneous application of NGF and electrical stimulation. There were significant increases in PC12 cell differentiation on the NGF-encapsulating rGO_{SH}/PMA_{SH} MS substrate compared with those on the non-NGF-encapsulating rGO_{SH}/PMA_{SH} MS substrate after 2, 4, or 7 days of culture. PC12 cells were exposed to a constant voltage of 1 V for 1 h each day ($N = 5$; $^{*}P < 0.05$, $^{**}P < 0.01$ was considered statistically significant) (E +: with electrical stimulation; E –: without electrical stimulation).

with electrical stimulation was 8.9, whereas the cell viability on the rGO_{SH}/PMA_{SH} MS substrate without electrical stimulation was 8.5. These results suggest that the amount of NGF does not play an important role in the viability of PC12 cells. In contrast, for the non-NGF-encapsulating rGO_{SH}/PMA_{SH} MS substrate, the cell viability was significantly different in response to 4d E– and 4d E+ versus 7d E– and 7d E+. This result suggests that electrical stimulation can increase PC12 cell viability on the non-NGF rGO_{SH}/PMA_{SH} MS substrate ($P < 0.05$).

PC12 cells with their neurite outgrowth length were significantly increased ($P < 0.05$) on the NGF@rGO_{SH}/PMA_{SH} MS substrate compared with those on the non-NGF@rGO_{SH}/PMA_{SH} MS substrate in response to 2d E+ or 2d E– as shown in Figure 8b,c. Additionally, following 2 days of electrical stimulation, the neurite outgrowth of PC12 cells was greater than that of cells that were not exposed to an electrical stimulus.

When we observed the neurite length at 4 days, as shown in Figure 8b, this parameter increased dramatically, from 80 μm to 145 μm, with electrical stimulation. At the same time, the percentage of cells with neurites, as shown in Figure 8c, was enhanced from 33% to 85% because of an 86-ng increase in NGF release in response to electrical stimulation. During 1 week of co-culture, the percentage of cells with neurites and the neurite length were also increased. Moreover, the non-NGF-encapsulating rGO_{SH}/PMA_{SH} MS substrate under the same condition was used as the control group. Smaller increases in neurite length and the percentage of cells with neurites were found on the non-NGF-encapsulating rGO_{SH}/PMA_{SH} MS substrate compared with those on the NGF-encapsulating rGO_{SH}/PMA_{SH} MS substrate. For the non-NGF-encapsulating rGO_{SH}/PMA_{SH} MS substrate, the neurite length was 1 ± 0.3 μm, 66 ± 5 μm, 2 ± 0.35 μm, 111 ± 11 μm, 5 ± 2 μm, and 150 ± 16 μm for samples 2d E–, 2d E+, 4d E–, 4d E+, 7d E-, and 7d E+, respectively, as shown in Figure 8b. In Figure 8c, we also observed that the percentage of cells with neurites was $2 \pm 0.4\%$, $18 \pm 2.3\%$, $3 \pm 1\%$, $66 \pm 4\%$, $5 \pm 3\%$, and $85 \pm 3\%$ for samples 2d E–, 2d E+, 4d E–, 4d E+, 7d E–, and 7d E+, respectively, for the non-NGF-encapsulating rGO_{SH}/PMA_{SH} MS substrate. The neurite length and the percentage of cells with neurites were statistically significantly different ($P < 0.05$) between NGF and non-NGF encapsulation rGO/PMA MS substrates. The above reported data demonstrate that both NGF and electrical stimulation show obvious effects on PC12 cell differentiation; nevertheless, the contribution from NGF release has a greater effect on neurite length and the percentage of PC12 cells with neurites during a longer duration (7 days) of cell culture compared to that from electrical stimulation.

3. Conclusion

In summary, we have developed multifunctional microcapsules to encapsulate NGF by functionalizing the thiol groups on the surface of rGO nanosheets and depositing self-assembled rGO_{SH}/PMA_{SH} LbL onto the MS. The stimulus-responsive, well-ordered rGO_{SH}/PMA_{SH} microcapsules with microscale topography were arrayed into a 3-D extracellular matrix on a flexible ITO substrate. The goal was to accelerate the proliferation and differentiation of PC12 cells by controlling NGF release behavior and manipulating rGO_{SH}/PMA_{SH} microcapsule interfaces during electrical stimulation. Our results show that a combination of surface topography, a chemical cue, and electrical stimulation not only has a positive effect on cell viability but also strongly enhances the neurite outgrowth of PC12 cells. This biocompatible and conductive rGO_{SH}/PMA_{SH} microcapsule can also be integrated into a patterned substrate to provide a new platform for tissue engineering applications.

4. Experimental Section

Materials: Graphite with an average mesh size of 325 and a purity of 99.8 mol% was supplied by Alfa Aesar. Concentrated sulfuric acid (95-97 mol% H_2SO_4), nitric acid (69–70 mol% HNO_3), potassium chlorate and phosphate-buffered saline (PBS) (pH 7), used for the preparation of buffers, were purchased from Sigma-Aldrich Co. Mesoporous silica (MS) (3-μm diameter, pore size = 2 nm) was used as a core. Poly(methacrylic acid, sodium salt) (PMA) (MW = 15000 g/mol) was purchased from Polysciences (USA), and dithiothreitol (DTT), *N*-chloro-*p*-toluenesulfonamide sodium salt (chloramine T), 2-hydroxy-2-methyl-propiophenone (Darocur 1173), cysteamine hydrochloride, 5,5′-dithiobis-2-nitrobenzoic acid (Ellman's reagent), 2-hydroxyethyl methacrylate (HEMA), and 3-aminopropyltrimethoxysilane (APS) were purchased from Sigma-Aldrich. Fluorescein isothiocyanate (FITC) (MW = 389.382 g mol^{-1}; Sigma) and rhodamine B isothiocyanate (RITC) (W = 536.08 g/mol; Fluka) were used as an MS core-shell dye. NGF 2.5S (26 kDa, male mice; Invitrogen) was used as a model drug to characterize the release behavior. An NGF enzyme-linked immunosorbent assay (ELISA) kit was obtained from ChemiKine™ to measure the amount of NGF.

Preparation of Mesoporous SiO_2^+ Particles: A suspension of 3-μm-diameter SiO_2 particles dispersed in 1 mL of ethanol was reacted with 250 μL of APS and 50 μL of 30% ammonia solution for 2 h. Next, the particles were washed several times in ethanol and then three times in distilled water. The resulting particles had a ξ-potential of 45 ± 3 mV, as measured in 10 mM sodium acetate buffer (pH 4).

NGF Loading into the Mesoporous SiO_2^+ Particles: The mesoporous SiO_2^+ particles were washed with PBS (pH 5) and then washed with deionized water. NGF (150 ng mL^{-1}) was dissolved in PBS (pH 7.4) in advance. The NGF was loaded into the mesoporous SiO_2^+ particles by exposing the particles to the NGF solution for 12 h followed by washing with water. The NGF diffused into the microcapsules in the pH 7.4 buffer solution.

Preparation of PMA_{SH}: PMA solution (250 mg of 30 wt% solution) was diluted with 5 mL of potassium phosphate buffer (0.1 M, pH 7.2). The resulting solution was charged with EDC (70 mg) and NHS (45 mg), and the mixture was stirred for 15 min. Next, cysteamine dihydrochloride (7.5 mg, target modification 20 mol%), which had been preoxidized in air for several days, was added to the mixture, and the reaction was allowed to proceed overnight. The resulting mixture was dialyzed extensively against distilled water, and the polymer was isolated via freeze drying. The resulting solid was purified further by reprecipitation from water into dioxane.[25] A PMA sample with thiol groups at 6.125 mol% was synthesized from PMA and cysteamine dihydrochloride via carbodiimide coupling.[26] Fluorescence labeling of PMA_{SH} was performed using a 1 g L^{-1} dimethylsulfoxide (DMSO) solution of FITC (typically 10 μg) mixed with 1–10 mg of PMA_{SH} at a concentration of 10 g L^{-1} in pH 7.2 phosphate buffer. The reaction between the maleimide in the fluorescent dye and the thiol groups along the polymer was allowed to proceed overnight; then, the polymer was purified *via* gel filtration and isolated via freeze drying. The PMA_{SH} was incubated in a solution of 100 g L^{-1} DTT at pH 8 for at least 12 h and diluted with 10 mM sodium acetate buffer (pH 4) to the required concentration.

Preparation of rGO_{SH}: Graphite oxide (GO) was prepared from natural graphite powder by oxidation with potassium chlorate according

to a modification of Hummers' method.[27] Sonication promotes the exfoliation of stacked GO sheets in oxidized graphite. Centrifugation allows the separation of large and small size graphene sheets. rGO sheets of an average size of 200 nm were obtained after sonication for 30 min, and centrifugation at 12 000 rpm was repeated three times. The size of the rGO sheets was determined by dynamic light scattering (DLS), and the results are presented in Figure S1, Supporting Information. The small-sized rGO sheets were thiol functionalized by reacting with cysteamine in ethanol suspension with the aid of the condensation agent dicyclohexylcarbodiimide (DCC). In a typical procedure, functionalized rGO was added to ethanol at 0.3 mg mL^{-1} and sonicated for 10 min. An excess (relative to the calculated amounts of carboxylic groups present on the rGO) of DCC ethanolic solution (0.5 mg mL^{-1}) was added, and the solution was stirred for several minutes. Finally, 5 mM cysteamine solution was added, and the mixture was stirred again for 24 h at room temperature. The amount of cysteamine was double the amount that was estimated for the carboxylic groups. The thiol-functionalized rGO obtained was relatively unstable and tended to precipitate slowly after the reaction. The precipitate obtained after the reaction was separated from the solution by filtration and washed to remove unreacted molecules; the byproducts were then dispersed in ethanol by prolonged sonication (30 min).

Assembly of rGO_{SH}/PMA_{SH} LbL MS: A suspension of the SiO_2^+ particles (0.25 wt%) was washed with pH 4 buffer via several water centrifugation/redispersion cycles. The resulting suspension was combined with an equal volume (1 mL) of a 1 mg mL^{-1} solution of rGO_{SH} (thioled graphene) in 10 mM sodium acetate buffer, pH 4, and adsorption of the rGO_{SH} was allowed to proceed for 15 min with constant shaking. Next, the particles were washed with fresh pH 4 buffer (three times), redispersed, and used in 1 µL of solution that was combined with 2 µL of reduced PMA_{SH} in 10 mM sodium acetate buffer to a final concentration of PMA_{SH} of 0.186 g mL^{-1}. PMA_{SH} adsorption was allowed to proceed for 15 min, after which the particles were washed with fresh 10 mM acetate buffer, pH 4. This procedure describes the assembly of a single bilayer, and the process was repeated until the desired number of bilayers was assembled. In this study, the PMA_{SH}/rGO_{SH} LbL structure was designed to have 6 bilayers of PMA_{SH}/rGO_{SH}, and its outermost layer was a PMA_{SH}. The particles were treated with a solution of chloramine T (2.5 mM) in 2-(*N*-morpholine) ethane sulfonic acid (MES) buffer solution (50 mM, pH 6) for 1 min; this was followed by two washing cycles with MES buffer solution and sodium acetate buffer solution (20 mM, pH 4) to achieve the oxidation of thiol groups into disulfide linkages between the PMA_{SH} and thioled graphene layers. After forming the disulfide bonds, the coating layers outside the core were stabilized. The rGO_{SH}/PMA_{SH} LbL MS, as synthesized above, was deposited onto an indium tin oxide (ITO, or tin-doped indium oxide)-coated conducting flexible plate (PET substrate, JoinWill Tech. Co., Ltd., Taiwan; electrical resistance of sq/50 Ω) with dimensions of 20 mm × 20 mm × 0.02 mm. We used the HEMA to fix the microcapsules on the ITO substrate to form 3D arrays by free-radical photopolymerization.

Determination of the Thiol Group Content: The thiol content of the resulting polymer was characterized using Ellman's reagent.[26] The degree of modification, that is, the number of thiol groups immobilized on the PMA, was determined spectrophotometrically with Ellman's reagent. First, 0.50 mg of conjugate was hydrated in 250 µL of demineralized water. Then, 250 µL of phosphate buffer (0.5 M, pH 8.0) and 500 µL of Ellman's reagent (3 mg) in 10 mL of 0.5 M phosphate buffer, pH 8.0) were added. The samples were incubated for 3 h at room temperature. The supernatant was separated from the precipitated polymer by centrifugation (10 000*g*, 10 min). Thereafter, 300 µL of the supernatant was transferred to a microtitration plate and subjected to an ELISA, and the absorbance was measured at a wavelength of 412 nm (DV990BV4, GDV). A cysteamine standard curve was used to calculate the number of thiol groups immobilized on the polymer.

Morphology of the rGO_{SH}/PMA_{SH} LbL MS: The microcapsules were visualized using an optical microscope (OM), whereas the surface morphology and diameter of the rGO_{SH}/PMA_{SH} LbL MS were examined using scanning electron microscopy (SEM) (JEOL JSM S6700, JEOL Ltd., Akishima-shi, Japan). For SEM analysis, the microcapsules were fixed on a 0.5 cm × 0.5 cm silicon wafer and then critical-point dried. Finally, the microcapsules were coated with an ultrathin layer of platinum and examined by SEM under operation at an accelerating voltage of 15 kV. Furthermore, to investigate the thickness of the six-layer rGO_{SH}/PMA_{SH} LbL coating on the MS, photoluminescence (PL) microscopy was used. RITC (MW = 536.08 g mol^{-1}, Fluka) and FITC-dextran (MW = 389.382 g mol^{-1}, Sigma) were used to tag the MS core and the PMA_{SH} layer, respectively, which allowed for microcapsule visualization under a PL microscope by sharply defining the inner and outer perimeters of the LbL microcapsule.

Study of NGF Release from the rGO_{SH}/PMA_{SH} MS Substrate: NGF@rGO_{SH}/PMA_{SH} MS substrates ($N = 5$) were placed into a six-well culture dish with a well size of 20 mm and incubated in PBS for 7 days at 37 °C. Similarly, NGF@rGO_{SH}/PMA_{SH} MS substrates ($N = 5$) in a six-well culture dish with an electrical stimulation setup, as shown in Figure S9 (Supporting Information), were incubated under the same conditions. In total, 10 µL of supernatant was collected from each well at each time point and analyzed with a commercially available sandwich ELISA kit. An NGF ELISA (Catalog No.: CYT304, ChemiKine™, USA and Canada) was performed strictly in accordance with the manufacturer's manual to examine the concentration of NGF released from the rGO_{SH}/PMA_{SH} MS substrate into the PBS. The ELISA for NGF expression involved the measurement of the change in optical density (OD), which was proportional to the NGF concentration, with a linear standard curve from 7.8–500 pg mL^{-1} ($R^2 = 0.997$, $P \leq 0.001$).[28] In this study, supernatants were directly added to a 96-well ELISA microtiter plate in a buffer provided with the kit, after which the NGF ELISA was performed as previously described. Finally, the absorbance at 450 nm (Sunrise Absorbance Reader, Tecan Group Ltd., Switzerland) was used to calculate the NGF concentration present in each sample. Each NGF release experiment was performed in triplicate.

Cell Culture on the Test Substrates: The PC12 cell line (ATCC), derived from a rat pheochromocytoma of adrenal medullary origin,[29] has been extensively used as a model system for neuronal differentiation. PC12 cells stop dividing and terminally differentiate when treated with NGF (Sigma). The 3-(4, 5-dimethylthiazol-2-yl)-2, 5-diphenyltetrazolium bromide (MTT) assay was used to compare the cell viability of an ITO substrate, an MS substrate, and the rGO_{SH}/PMA_{SH} microcapsule substrate. Cells were cultured in 75-cm^2 flasks at a density of 10 000 cells cm^{-2} and maintained in culture until the plates reached > 95% confluence. The PC12 cells were maintained in Dulbecco's modified Eagle's medium (DMEM) (Invitrogen) supplemented with 85% RPMI 1640, 2 mM L-glutamine (Gibco), 10% heat-inactivated horse serum (Gibco), and 5% fetal bovine serum (Gibco) at incubator settings of 5% CO_2 and 37 °C. In all experiments, cells were harvested from subconfluent cultures using trypsin and were then resuspended in fresh complete medium before plating. A comparison of the in vitro cell viability and proliferation on the ITO, MS, and rGO_{SH}/PMA_{SH} MS microcapsule substrates over time was performed for PC12 cells. Briefly, 2×10^5 cells were plated in six-well plates in 1 mL of culture medium for 12 h or 48 h. At the end of the incubation, 100 µg of MTT solution was added and incubated for an additional 4 h. The medium was then replaced with 1 mL of DMSO. In total, 200 µL of the mixed solution was added to a 96-well plate to monitor the absorbance at a wavelength of 570 nm using a Sunrise absorbance microplate reader (CTECAN). The OD of the media was proportional to the number of viable cells. The media were changed every 2 days. All experiments were performed in triplicate.

Neurite Formation Observation and Assay: The PC12 cells cultured on the ITO, MS, or rGO_{SH}/PMA_{SH} MS microcapsule substrates were fixed in 3.7% formaldehyde in PBS for 30 min and permeabilized in 0.1% Triton X-100 for 30 min in 37 °C. The cell nuclei were visualized by incubation for 30 min with 200 ng mL^{-1} 4′,6-diamidino-2-phenylindole (DAPI) (Sigma). The actin cytoskeleton was stained with a secondary goat anti-mouse IgG1 Alexa Fluor 488 antibody (Invitrogen, Darmstadt, Germany) overnight, and each step was washed with PBS three times. Morphological changes in the PC12 cells were observed and photographed using confocal laser scanning microscopy (CLSM). Ten

fluorescence images were taken of randomly selected areas in each substrate. To quantify the number of neurite-bearing cells and their neurite length on each substrate, ImageJ software was used (NIH ImageJ ver.1.42, National Institutes of Health, Bethesda, MD, USA). The neurite length of PC12 cells was defined as the distance from the tip of a neurite to the junction between the neurite base and the cell body; the value was expressed relative to the respective cell soma. Each experiment was independently repeated five times for each substrate. For statistical analyses, the Wilcoxon rank sum test or the two-tailed unpaired Student *t*-test was performed using the SPSS software package (version 13.0). A *P*-value < 0.05 was considered to be statistically significant. All data are presented as the mean value ± SEM ($N = 5$).

Supporting Information

Supporting Information is available from the Wiley Online Library or from the author.

Acknowledgments

This work was financially supported by the National Science Council of the Republic of China, Taiwan under Contract of NSC 102-2221-E-009 -023-MY3 and NSC100-2320-B-009-006-MY2 and by the "Aim for the Top University" program of the National Chiao Tung University and the Ministry of Education, Taiwan, R.O.C.

Received: November 13, 2013
Revised: January 29, 2014
Published online: March 4, 2014

[1] a) N. Gomez, J. Y. Lee, J. D. Nickels, C. E. Schmidt, *Adv. Funcl Mater.* **2007**, *17*, 1645; b) J. D. Foley, E. W. Grunwald, P. F. Nealey, C. J. Murphy, *Biomaterials* **2005**, *26*, 3639; c) W.-T. Su, Y.-F. Liao, T.-W. Wu, B.-J. Wang, Y.-Y. Shih, *J. Biomed. Mater. Res. Part A* **2013**, *101A*, 185; d) S. Schlie-Wolter, A. Deiwick, E. Fadeeva, G. Paasche, T. Lenarz, B. N. Chichkov, *ACS Appl. Mat. Interfaces* **2013**, *5*, 1070.
[2] N. Gomez, Y. Lu, S. Chen, C. E. Schmidt, *Biomaterials* **2007**, *28*, 271.
[3] K. Kang, S.-E. Choi, H. S. Jang, W. K. Cho, Y. Nam, I. S. Choi, J. S. Lee, *Angew. Chem. Int. Ed.* **2012**, *51*, 2855.
[4] a) P. Roach, T. Parker, N. Gadegaard, M. R. Alexander, *Surf. Sci. Rep.* **2010**, *65*, 145; b) A. Khademhosseini, R. Langer, J. Borenstein, J. P. Vacanti, *Proc. Natl. Acad. Sci. U. S. A.* **2006**, *103*, 2480; c) I. Armentano, M. Dottori, E. Fortunati, S. Mattioli, J. M. Kenny, *Polym. Degrad. Stab.* **2010**, *95*, 2126; d) M. J. P. Biggs, R. G. Richards, M. J. Dalby, *Nanomedicine* **2010**, *6*, 619.
[5] a) C. D. McCaig, A. M. Rajnicek, B. Song, M. Zhao, *Trends Neurosci.* **2002**, *25*, 354; b) M. Wood, R. K. Willits, *Bioelectromagnetics* **2006**, *27*, 328; c) J. S. Park, K. Park, H. T. Moon, D. G. Woo, H. N. Yang, K.-H. Park, *Langmuir* **2008**, *25*, 451.
[6] S. Agarwal, X. Zhou, F. Ye, Q. He, G. C. K. Chen, J. Soo, F. Boey, H. Zhang, P. Chen, *Langmuir* **2010**, *26*, 2244.
[7] N. Gomez, C. E. Schmidt, *J. Biomed. Mater. Res. Part A* **2007**, *81A*, 135.
[8] H. J. Chung, T. G. Park, *Adv. Drug Delivery Rev.* **2007**, *59*, 249.
[9] X. Xu, W.-C. Yee, P. Y. K. Hwang, H. Yu, A. C. A. Wan, S. Gao, K.-L. Boon, H.-Q. Mao, K. W. Leong, S. Wang, *Biomaterials* **2003**, *24*, 2405.
[10] K. Moore, M. Macsween, M. Shoichet, *Tissue Eng.* **2006**, *12*, 267.
[11] A. K. Geim, K. S. Novoselov, *Nat. Mater.* **2007**, *6*, 183.
[12] a) J. Hong, J. Y. Han, H. Yoon, P. Joo, T. Lee, E. Seo, K. Char, B.-S. Kim, *Nanoscale* **2011**, *3*, 4515; b) J. Hong, K. Char, B.-S. Kim, *J. Phys. Chem. Lett.* **2010**, *1*, 3442.
[13] S. A. Ju, K. Kim, J.-H. Kim, S.-S. Lee, *ACS Appl. Mat. Interfaces* **2011**, *3*, 2904.
[14] A. Kikuchi, T. Okano, *Adv. Drug Delivery Rev.* **2002**, *54*, 53.
[15] a) A. L. Becker, A. N. Zelikin, A. P. R. Johnston, F. Caruso, *Langmuir* **2009**, *25*, 14079; b) A. D. Price, A. N. Zelikin, Y. Wang, F. Caruso, *Angew. Chem. Int. Ed.* **2009**, *48*, 329; c) Y. Yan, A. P. R. Johnston, S. J. Dodds, M. M. J. Kamphuis, C. Ferguson, R. G. Parton, E. C. Nice, J. K. Heath, F. Caruso, *ACS Nano* **2010**, *4*, 2928.
[16] C.-Y. Su, Y. Xu, W. Zhang, J. Zhao, X. Tang, C.-H. Tsai, L.-J. Li, *Chem. Mater.* **2009**, *21*, 5674.
[17] G. Kang, R. Ben Borgens, Y. N. Cho, *Langmuir* **2011**, *27*, 6179.
[18] a) S. L. Bechara, A. Judson, K. C. Popat, *Biomaterials* **2010**, *31*, 3492; b) S. Berski, J. van Bergeijk, D. Schwarzer, Y. Stark, C. Kasper, T. Scheper, C. Grothe, R. Gerardy-Schahn, A. Kirschning, G. Drager, *Biomacromolecules* **2008**, *9*, 2353; c) S. Agarwal, X. Z. Zhou, F. Ye, Q. Y. He, G. C. K. Chen, J. Soo, F. Boey, H. Zhang, P. Chen, *Langmuir* **2010**, *26*, 2244.
[19] a) G. Cellot, E. Cilia, S. Cipollone, V. Rancic, A. Sucapane, S. Giordani, L. Gambazzi, H. Markram, M. Grandolfo, D. Scaini, F. Gelain, L. Casalis, M. Prato, M. Giugliano, L. Ballerini, *Nat. Nanotechnol.* **2009**, *4*, 126; b) M. K. Gheith, V. A. Sinani, J. P. Wicksted, R. L. Matts, N. A. Kotov, *Adv. Mater.* **2005**, *17*, 2663.
[20] Y. Wang, W. C. Lee, K. K. Manga, P. K. Ang, J. Lu, Y. P. Liu, C. T. Lim, K. P. Loh, *Adv. Mater.* **2012**, *24*, 4285.
[21] S. Y. Park, J. Park, S. H. Sim, M. G. Sung, K. S. Kim, B. H. Hong, S. Hong, *Adv. Mater.* **2011**, *23*, H263.
[22] a) K. Kimura, Y. Yanagida, T. Haruyama, E. Kobatake, M. Aizawa, *Med. Biol. Eng. Comput.* **1998**, *36*, 493; b) L. F. Jaffe, M.-M. Poo, *J. Exp. Zool.* **1979**, *209*, 115; c) L. Erskine, C. D. McCaig, *Dev. Biol.* **1995**, *171*, 330; d) C. D. McCaig, L. Sangster, R. Stewart, *Dev. Dynam.* **2000**, *217*, 299; e) A. E. Wilkinson, A. M. McCormick, N. D. Leipzig, *Synth. Lect. Tissue Eng.* **2011**, *3*, 1.
[23] Y. Cho, R. Shi, A. Ivanisevic, R. Ben Borgens, *Nanotechnology* **2009**, *20*, 4484.
[24] G. Kang, R. B. Borgens, Y. Cho, *Langmuir* **2011**, *27*, 6179.
[25] A. N. Zelikin, J. F. Quinn, F. Caruso, *Biomacromolecules* **2005**, *7*, 27.
[26] M. Werle, M. Hoffer, *J. Controlled Release* **2006**, *111*, 41.
[27] H. A. Becerril, J. Mao, Z. Liu, R. M. Stoltenberg, Z. Bao, Y. Chen, *ACS Nano* **2008**, *2*, 463.
[28] M. A. Vizzard, *Exp. Neurol.* **2000**, *161*, 273.
[29] L. A. Greene, A. S. Tischler, *Proc. Natl. Acad. Sci. U. S. A.* **1976**, *73*, 2424.